Vol. 12, No. 4, 2021
ISSN 2233-4203/ e-ISSN 2093-8950
ARTICLE www.msletters.org | Mass Spectrometry Letters

Ion Mobility Signatures of Glutamine-Containing Tryptic Peptides in the Gas Phase

Hyun Hee L. Lee[1]*, Soo Yeon Chae[2], Myung Kook Son[2], and Hugh I. Kim[2]*

[1]*Research Division of Food Functionality, Korea Food Research Institute, Jeollabuk-do 55365, Republic of Korea*
[2]*Department of Chemistry, Korea University, Seoul 02841, Republic of Korea*

Received October 28, 2021; Revised November 30, 2021; Accepted November 30, 2021
First published on the web December 31, 2021; DOI: 10.5478/MSL.2021.12.4.137

Abstract : Herein we report multiple ion mobility (IM) peaks in electrospray ionization IM mass spectrometry (ESI-IM-MS) produced by glutamine residue in peptide. The mobility features of 147 peptides were investigated using ESI-IM-MS combined with liquid chromatography. Of these peptides, 66 presented multiple IM peaks, and analysis of their sequence using collision induced dissociation (CID) revealed that glutamine (Gln), as well as proline (Pro), plays a critical role in generating multiple IM peaks. Mutant-based investigations using Gln-containing peptides indicate that the side chain of Gln promotes intermolecular interactions, inducing multiple structures of the peptide ions in the gas phase. Consequently, the present study demonstrates that the distinct ion mobility signatures identified herein can potentially be used to characterize glutamine-containing peptide ions.

Keywords : ion mobility mass spectrometry, tryptic peptide, ion chemistry, glutamine

1. Introduction

Ion mobility mass spectrometry (IM-MS), coupled with electrospray ionization (ESI), using two-dimensional separation based on the mass-to-charge ratio (*m*/*z*) and collision cross section (CCS) of conformational ensembles in the gas phase, is now widely utilized for analyzing various biomolecules.[1-4] By interfacing this setup with liquid chromatography (LC), which can provide additional separation prior to the implementation of IM-MS, more precise determination of the analyte peak ions in MS spectra can be accomplished.[5] Therefore, a number of researchers have employed IM-MS to characterize various compounds, including peptides, proteins, carbohydrates, lipids, and pharmaceuticals.[3,4,6] Notably, the unique separation ability of IM-MS has been extensively utilized for proteomic analysis,[7,8] along with characterization of the structural features of small peptides in the gas phase.[1,4,9-11]

Clemmer and co-workers pioneered investigations of the distinctive mobility features associated with the primary structures of peptide ions.[12,13] Among the 20 biotic amino acids, the unique characteristics of the proline (Pro) reside can induce multiple gas phase conformations of peptides, resulting in multiple IM peaks.[12,13] A series of studies reported that cis-trans isomerizations of proline lead to multiple conformations of peptides in the gas phase.[10,12,14-16] It is currently widely accepted that multiple IM peaks of peptide ions may be a signature of proline residues in the peptide. Since there has been growing interest in the use of IM-MS in peptide and proteome analysis, investigating additional factors that can induce multiple conformations of peptides in the gas phase, which can result in broadening of the peaks or multiple peaks in the IM spectra.

Herein, we demonstrate that glutamine (Gln) residues in peptide ions play a significant role in inducing multiple structures of the peptides during transfer from solution to the gas phase during ESI. 147 tryptic digested peptides were investigated using two different IM-MS instruments, and the IM-MS results show that Gln is the second most abundant residue on the peptide ions with multiple IM peaks. Then, IM-MS experiments and molecular dynamics (MD) simulations using model peptides were further performed to reveal the effect of the Gln residue on the distinct IM features of the peptides.

Open Access
*Reprint requests to Hyun Hee L. Lee, Hugh I. Kim
https://orcid.org/0000-0001-9205-1806 (Kim),
https://orcid.org/0000-0003-2161-5402 (Lee)
E-mail: hughkim@korea.ac.kr; hyunheelee@kfri.re.kr

This Article is dedicated to Professor Seung Koo Shin in commemorating his retirement and contribution to the Korean Society for Mass Spectrometry.

Experimental

Chemicals and reagents

Bovine fetuin (bF), bovine transferrin (bT), human transferrin (hT), and human α-acid glycoprotein (hAGP) were purchased from Sigma-Aldrich (St. Louis, MO, USA). Human secreted frizzled-related protein 4 (sFRP4) was purchased from Sino Biological (Beijing, China). Trypsin and N-glycosidase F (PNGase F) were purchased from Promega Corporation (Madison, WI, USA). 1,4-Dithiothreitol (DTT) was purchased from LPS Solution (Daejeon, Republic of Korea). Iodoacetamide (IAM), ammonium bicarbonate (ABC), formic acid (FA), and poly-DL-alanine were purchased from and Sigma-Aldrich. All peptides, in which glutamine in their sequence was substituted by glycine, were purchased from Anygen (Gwangju, Korea). HPLC-grade water and acetonitrile were purchased from JT Baker (Philipsburg, NJ, USA). Oasis HLB cartridges were purchased from Waters (Milford, MA, USA).

Tryptic digestion of proteins

100 μg of the proteins was dissolved in 200 μL of 50 mM ABC buffer. 10 mM DTT and 30 mM IAM dissolved in the ABC buffer were utilized to reduce the disulfide bonds and prevent the formation of disulfide bonds, respectively. The denatured protein solutions were incubated with 10 μg of trypsin in the ABC buffer at 37°C for 24 h. For increasing the sequence coverages, deglycosylation of the glycopeptides in trypsin digests was performed by incubating the digests with 50 u of PNGase F at 37°C for 24 h. Purification and enrichment of the peptides were performed using Oasis HLB cartridges. Before injecting the peptide solution into the cartridge, the cartridge was washed with 1 mL of HPLC ACN and conditioned with 2 mL of HPLC water. After injection, the peptides retained in the cartridge were sequentially eluted with 2 mL of HPLC water and 1 mL of 50% ACN. Each eluent was lyophilized, and then dissolved in 200 μL of HPLC water with 0.1% FA for the HPLC-MS experiments. The final concentrations of the peptides are approximately 6.6 μM or more and less than 23.2 μM.

High-performance liquid chromatography mass spectrometry (HPLC-MS) and collision-induced dissociation (CID)

All HPLC-MS/MS experiments for identifying the peptide sequences were performed in positive ion mode using an Agilent 6560 ion mobility quadrupole time-of-flight (IM-qTOF, Agilent Technologies, CA, USA) mass spectrometer with an electrospray ionization source. A 10 μL aliquot of the digested sample solutions was injected into the LC-MS equipped with an ACQUITY UPLC BEH Shield RP18 column (130 Å, 1.7 μm, 2.1 × 100 mm); 0.1% FA water (solvent A) and 0.1% FA ACN (solvent B) were utilized at a flow rate of 0.1 mL/min. The gradients for the two solvents were set as follows: 0–10 min, 0% B; 10–40 min, linear increase from 0 to 60% B; 40–45 min, linear increase from 60 to 90% B; 45–50 min, 90% B; 50−51 min, linear decrease from 90 to 0% B; 51–60 min, 0% B. For effective ionization of the peptides, the gas temperature, drying gas flow rate, and nebulizer pressure were set to 325°C, 3 L/min, and 20 psig, respectively. The sheath gas flow rate and temperature were set to 200°C and 8 L/min, respectively. The VCap, nozzle voltage, fragmentor voltage, and Oct 1 RF Vpp were also set to 3500 V, 2000 V, 350 V, and 700 V, respectively. The MS/MS spectra of ten major precursor ions in each cycle time were investigated by using implementing the auto MS/MS feature of the Agilent MassHunter Workstation Software (Agilent Technologies, CA, USA). The mass range for the MS/MS experiments was set as *m*/*z* 100–3000. Peptide identification was performed using MaxQuant software (version 1.5.8.3), and the PSM FDR, protein FDR, and site decoy fraction were set as 0.05, 0.05, and 0.01, respectively, for accurate identification.

Ion mobility mass spectrometry (IM-MS) and molecular dynamics (MD) simulations

Two ion mobility mass spectrometers (Waters Synapt G2-Si (Waters Corporation, Wilmslow, UK) and Agilent 6560 IM-qTOF) were utilized in the present study. For the Waters Synapt G2-Si instrument, the capillary voltage, source temperature, and desolvation temperature were set as 3.00 kV, 120°C, and 200°C, respectively. In addition, the cone gas flow, desolvation gas flow, and nebulizer gas flow were set as 40 L/h, 100 L/h, and 2.5 bar, respectively. The helium cell gas flow, IMS gas flow, IMS wave velocity, and IMS wave height of the Waters Synapt G2-Si instrument were adjusted to 180.00 mL/min, 60.00 mL/min, 650 m/s, and 40.0 V, respectively. For the Agilent 6560 instrument, the drift cell was filled with N_2 gas, and the pressure of the drift cell was set to 3.950 Torr. For data acquisition using the Agilent 6560 instrument, the frame rate, max drift time, and drift tube entrance voltage were set as 0.9 frames/s, 90 ms, and 1700 V, respectively. Additionally, we confirmed that the real funnel exit voltage, which can induce soft extraction condition to TOF, did not affect the distinct IM features of the peptides (Figure S1). The experimental collision cross-section (CCS) values from the data acquired with the Synapt G2-Si instrument were obtained by the calibration method developed by Thalassinos and coworkers[11] and the N_2-based CCS database developed by Bush and coworkers.[17] For Agilent 6560, the experimental CCS values were obtained by adjusting the drift tube entrance voltages, and we simultaneously utilized the Agilent ESI TOF tuning mix as an internal standard to minimize the CCS errors caused by the pressure fluctuation of the IM cell during the acquisition.

All MD simulations were performed using the GROMACS 4.5.5. package,[18,19] and the force field parameters of the peptide ions were acquired by using the CHARMM general force field (CGENFF) parameters.[20] We utilized Hyperchem 7.5 (Hypercube Inc., Gainesville, FL, USA) to construct the initial geometries of the protonated WC(WC1, WCAIGHQER; WC2, WCAIGHGER; WC3, WCVIGHQER), QD(QD1, QD GQFSVLFTK; QD2, GDGQFSVLFTK; QD3, QDGGFSVL FTK; QD4, GDGGFSVLFTK; QD5, QDGQFSALFTK), and HT(HT1, HTLNQIDSVK; HT2, HTLNGIDSVK; HT3, HTL NQIDSAK) ions and their peptide dimers. Especially, we placed two peptides so that two peptides are a cross and their functional groups face each other, for obtaining initial geometries of the dimers. Then, we sequentially performed energy minimization and simulated annealing of the structures. All simulated annealing processes were performed without restraining the structures. The 500 candidate structures of each peptide ion were obtained from simulated annealing (150 ns). Simulated annealing of all the peptide ions, except the QD1 dimers, was performed by varying the temperature between 300 K and 600 K, as reported in previous studies.[21,22] The peptide ions were heated from 300 to 600 K for 100 ps, equilibrated at 600 K for 150 ps, and then cooled to 300 K for 50 ps. Due to the weak inter/intramolecular interaction of the mutant peptide dimers, the temperature for the dimer ions was set between 450 and 500 K instead of 600 K. Before obtaining the final peptide structures, we confirmed that the peptide ions were sufficiently cooled after the simulated annealing processes (Figure S2). Ten representative structures were selected based on their potential energies, and their collision cross-section (CCS) was obtained using the Trajectory (TJ) model implemented in the MOBCAL program.[23]

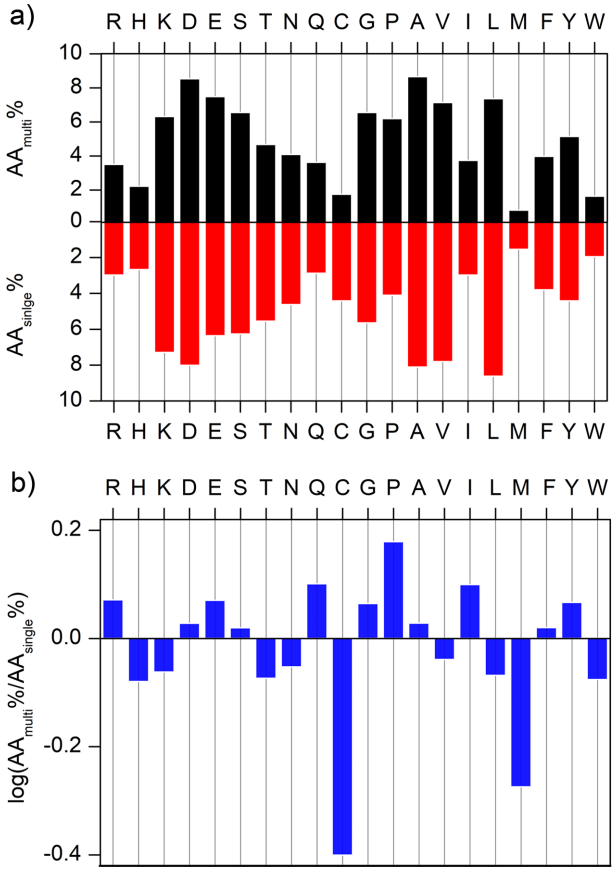

Figure 1. a) Proportion of each amino acid in the peptides having multiple IM peaks (black, AA_{multi}%) and those having single IM peaks (red, AA_{single}%) and b) logarithmic plot of AA_{multi}% and AA_{single}%.

Results and Discussion

Tryptic digests of five proteins, bovine fetuin, bovine transferrin, human transferrin, human α1-acid glycoprotein, and human secreted frizzled-related protein 4 (sFRP4), are investigated using Agilent 6560 LC-IM-MS. MS/MS experiments of the tryptic digests are further performed for sequence analysis prior to peptide IM studies. A total of 151 peptide ions (Table S1) was identified, and the ion mobility (IM) spectra of these peptides were investigated. Of the 151 identified peptide ions, the RPLC-IM-MS experiments provide IM spectra of 147 peptide ions (Tables S2 and S3). The mobility signatures of the 147 peptide ions show multiple IM peaks for 66 of these peptides (Tables S2 and S3, Figure S3−S6).

The charge states of the peptides with multiple IM peaks vary from +1 to +4. Among them, singly charged peptide ions are the most abundant (49.3%), and the population of peptides with multiple IM peaks was lower for the more highly charged peptides. The populations of doubly, triply, and quadruply charged peptide ions were 26.0, 19.2, and 5.5%, respectively. In contrast, single IM peaks were preferentially generated by peptides in the doubly charged state (59.6%), followed by those in the triply charged state (21.1%). These results suggest that peptides with multiple gas phase conformations preferentially adopt the singly charged state. However, there was no significant correlation between the peptide length and multiple IM peaks.

Our investigation on the primary structures (amino acid sequences) of peptides confirmed that a high abundance of the Pro residue in peptide ions leads to multiple IM peaks.[12] Figure 1 shows the difference in the proportion of 20 biotic amino acids for the peptide ions that generate multiple IM peaks and those that give rise to a single IM peak. Following Pro, Gln is the second most abundant amino acid residue, and 61.9% of the Gln-containing peptides investigated in the present study show multiple IM peaks. This result is highly notable because the Gln residue is unable to transform the peptide structures by isomerization, as in the case of the Pro residue. Basic and acidic amino acid residues, such as Arg and Glu, are also

frequently present in peptides with multiple conformations in the gas phase. This implies that the ability to generate electrostatic interactions between the amino acids may play an important role in the generation of multiple gas phase conformations.[24] The high proportions of hydrophobic amino acids, such as Gly, Ile, and Tyr, were estimated to be generated by the weak steric effects or weak electrostatic interactions.

The classification of the peptide ions with multiple IM peaks based on the distinct IM features provides further insights into understanding the contribution of the Gln residue toward the IM features of the peptide ions. As shown in IM spectra of the peptide ions with multiple IM peaks (Figure S3−S6), the peptide ions show several distinct characteristics on their IM spectra. First, some peptide ions have high-mobility IM peaks with at least 200% wide compared with the major IM peaks. Second, others of the peptide ions have high-mobility IM peaks partially overlapped with major IM peaks. Finally, others of the peptide ions have low-mobility IM peaks partially overlapped with major IM peaks. Based on the three distinct characteristics, we classified 66 peptides into three groups in order (A, B, and C; Table S2). The proportions of group A, B, and C were 60.0%, 22.9%, and 17.1%, respectively, and the overlapped portions of the three groups were excluded to obtain clear characteristics of each group.

Figure 2 provides overall information on the abundant amino acid (AA) residues, preferred peptide length, and preferred peptide charge of each group. To correctly decipher the characteristics of each group, we excluded the peptides having two or more IM features corresponding to the respective group. In the group with the highest proportion (group A), five AA residues are remarkably more abundant among the 20 AA residues (Figure 2a). Two of them are Pro and Gln, and the others are Tyr, Arg, and Gly. These results imply that Pro and Gln is significant to the formation of distinct IM features in group A, and the peptides in group A have abundant several residues available that can interact electrostatically with other portions of the peptides, or decrease steric effects for the interaction. However, the average peptide length in group

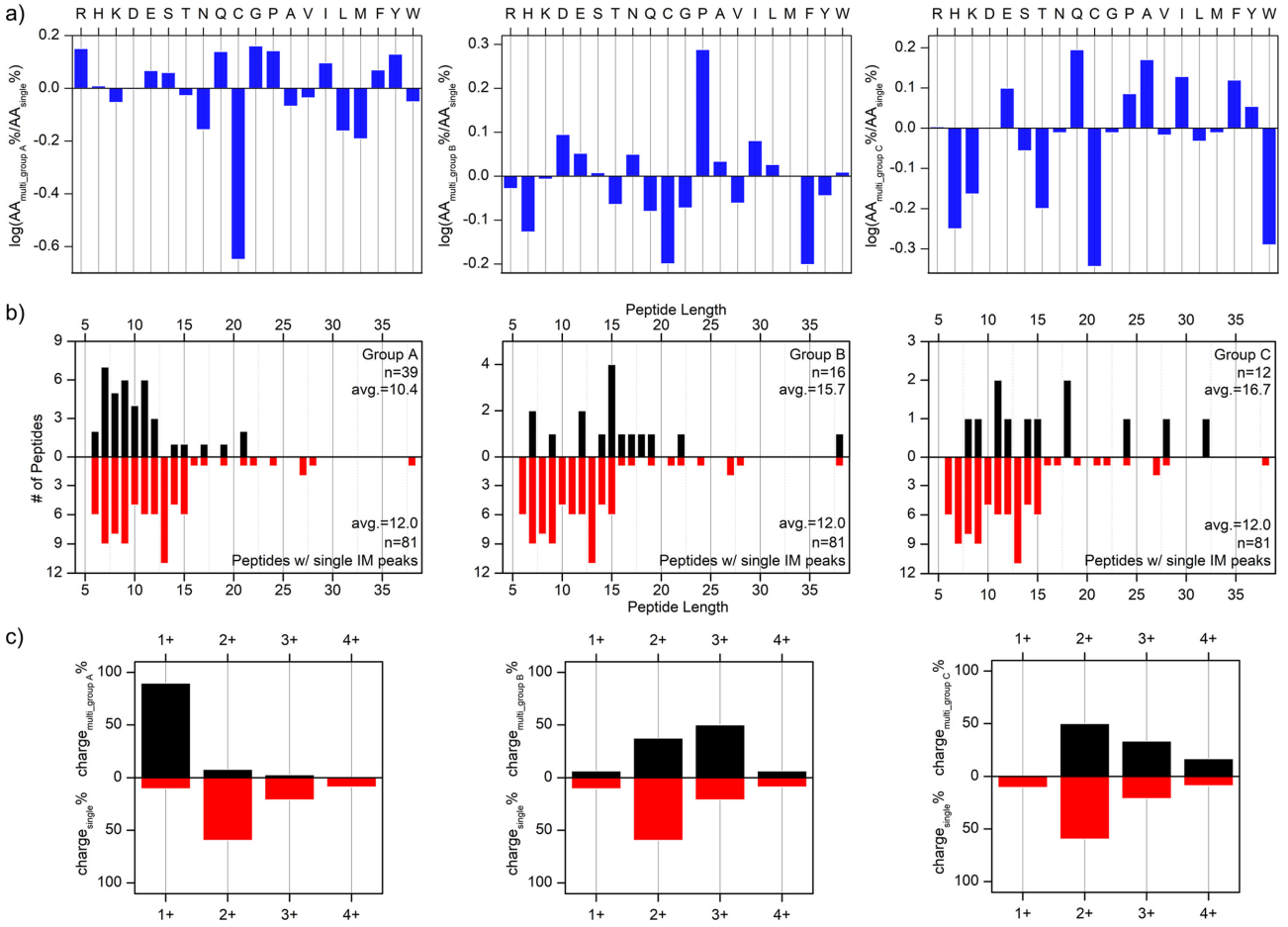

Figure 2. a) Logarithmic plot of amino acid proportions, b) peptide lengths, and c) peptide charge states of the peptides in group A (left), B (center), and C (right), along with those of the peptides with single IM peaks.

A is lower than the peptides with the single IM peaks, and most of the peptides in this group are singly charged peptides. These results suggest that group A has distinct characteristics that can make difficult to generate multiple structures of the peptides in the gas phase. In contrast to the group A, although several polar residues along with Pro and/or Gln are abundant in the group B and C (Figure 2a), the group B and C have longer peptide lengths than the peptides that have single IM peaks and higher charge states as compared with group A (Figure 2b). Thus, further investigation is required to reveal why distinct IM characteristics are generated in the peptides of group A.

To understand gas-phase characteristics of the group A peptides, IM-MS experiments were performed using Waters Synapt G2-Si with three peptides (WC1, QD1, and HT1; Figure 3a) from Group A (which has the highest

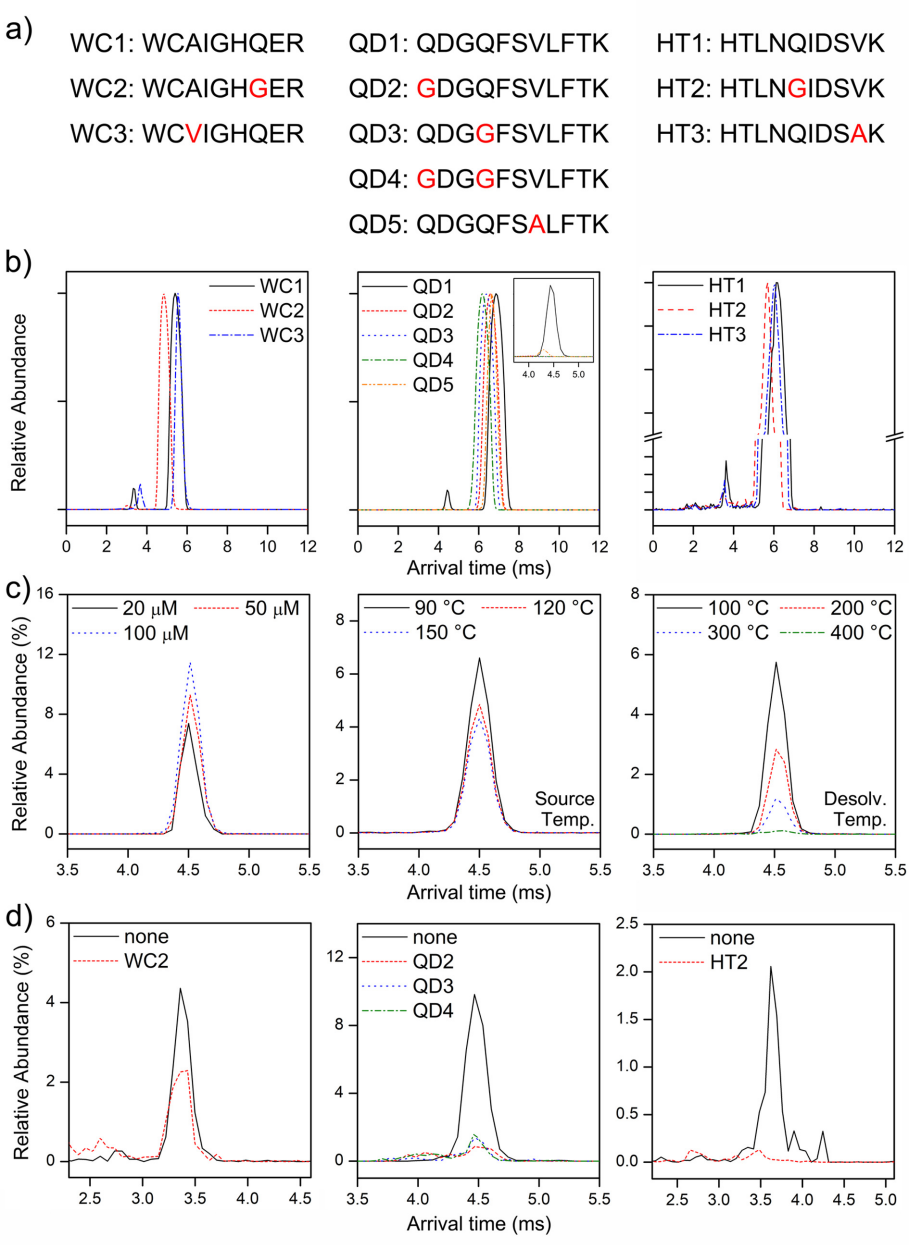

Figure 3. a) Peptide sequences, b) IM spectra of the peptides and their mutants, c) IM spectra of QD peptides depending on peptide concentration (left), source temperature (center), and desolvation temperature (right), and d) IM spectra of peptide mixtures. Each mutant peptide name in Figure 3d corresponds to WC1 (left), QD1 (center), and HT1 (right) solution (50 μM) mixed with the mutant peptide (50 μM). 'None' in Figure 3d corresponds to WC1 (left), QD1 (center), and HT1 (right) solution (50 μM). Full IM spectra of Figure 3c and 3d are presented in Figure S8.

proportion among the three groups) and their corresponding mutants, wherein the Gln residues were substituted by Gly (WC2, QD2, QD3, QD4, and HT2; Figure 3a) and the Ala or Val residues were substituted by Val or Ala (WC3, QD5, and HT3), respectively. For the selection of the model peptides, we first searched for Gln-containing peptides without Pro in group A, since IM features of group A are highly different with multiple IM peaks generated by Pro isomerization, and Gln is the most abundant residue in group A when excepting for Gly and Pro which can estimate their role in the formation of the multiple IM peaks. Then, three Gln-containing peptides were selected based on the average peptide lengths and preferred charge states in Group A. From the mass spectra, we confirmed that the WC1, QD1, and HT1 peptides predominantly formed singly protonated monomeric ions, (Figure S7), and the WC1, QD1, and HT1 ions showed two IM peaks (Figure 3b). The substitution of Gly for Gln reduces the abundance of high-mobility IM peaks. This clearly indicates that Gln plays a critical role in the generation of multiple IM peaks of peptides. The effects of Gln on the high-mobility IM peaks were also evaluated using mixtures of model peptides (WC1, QD1, and HT1) and their Gln→Gly mutants. The high-mobility IM peak abundances diminished for all the binary mixtures of the model peptide with the Gln→Gly mutants (Figure 3c and S8). The differences in the IM spectra of the peptides and their mutants depending on the peptide concentration and ionization parameters were then evaluated. Figure 3c, 3d, S9, and S10 show that the proportion of high-mobility IM peaks increased as the peptide concentration increased or the ionization parameters related only with temperature decreased, suggesting that weak intermolecular interactions of the peptide ions contribute to the generation of their high-mobility IM peaks. Consequently, our investigation using Gln-containing peptides implies that the peptide structures corresponding to the high-mobility IM peaks are strongly affected by the interactions between the peptides during the ESI process, and the conformation is constructed by weak noncovalent interactions. In addition, Gln residues play a critical role in the formation of the high-mobility structures.

Investigation of the gas-phase structures of the WC, QD, and HT peptide ions provides insight into the influence of Gln on the gas-phase structures of the peptide ions. We obtained 500 candidate structures for each peptide by performing molecular dynamics (MD) simulation, and selected ten representative structures having the lowest energy conformations among the candidate structures (Figure S11). The C-terminal i.e., Arg or Lys residue, which has a higher proton affinity than the other amino acid residues, was set as a protonated site.[25,26] We investigated all candidate structures in order to obtain representative structures with a theoretical CCS close to the experimental CCS of the singly protonated peptide monomer (Table S4). However, our simulated annealing could not generate a structure with a theoretical CCS close to the experimental CCS of the high-mobility IM peak. Figure 4a, 4b, and 4c show representative structures of the WC, QD, and HT peptide ions that correspond to the low-mobility IM peaks based on the theoretical CCS values, respectively. As gas-phase structures of peptide ions are commonly globular due to enhanced intramolecular electrostatic interactions in the gas phase,[27] the WC peptide ions also adopted globular shapes due to interactions between the polar functional groups (e.g., C-terminal residue and carbonyl backbone). The simulation also generated QD and HT peptide ions as overall globular structures. However, helical structural features were also found for the C-terminal region with Lys at the C-terminus.[28,29] Notably, the side chain of the Gln residues in both peptides do not participate in intramolecular electrostatic interactions. This implies that Gln does not directly participate in formation of the compact structure of the peptide in the gas phase. This raises the question of what structures of the peptide ions correspond to the high-mobility IM peak.

Based on our experimental observations and interpretations of the properties of the high-mobility IM peaks, along with the structures from MD simulations, it was hypothesized that the high-mobility structures may originate from intermolecular complexes. The highly charged peptide ions show higher mobility than those with low charge in the IM cell.[2,12] The experimental CCS values of the high-mobility IM peaks of WC1 and QD1, as doubly charged ions, were evaluated. These CCS values were then utilized for achieving representative structures of the dimer ions in the doubly charged state based on MD simulations. The theoretical CCS values of the doubly charged dimeric structures showed good agreement with the experimental CCS values of the doubly charged states corresponding to the high-mobility IM peaks ($\Delta CCS_{avg} \approx 6\%$, Table S5). The calculated structures of the peptide dimers provide additional information to support the formation of intermolecular peptide complexes. As shown in Figure 4d, the side chains of the Gln residues interact with the polar functional groups of the other peptides in the dimeric ion. In addition, the formation of hydrogen bonds between the amine group in the Gln side chain and the adjacent carbonyl backbone suggests that the Gln residues play a critical role in the formation of the dimer. These results suggest that multiple noncovalent interactions of the Gln residues in the peptide ion induce the formation of complex ions that give rise to the high-mobility IM peaks. However, the present mass spectral analysis indicates that WC1 and QD1 were observed as singly charged monomeric species. Thus, it is suggested that a peptide complex ion in higher charged states (e.g. doubly charged dimer) is formed during the ESI process, the structure of which is disrupted during transfer from the IM cell to the mass analyzer. Further MS experiments provided

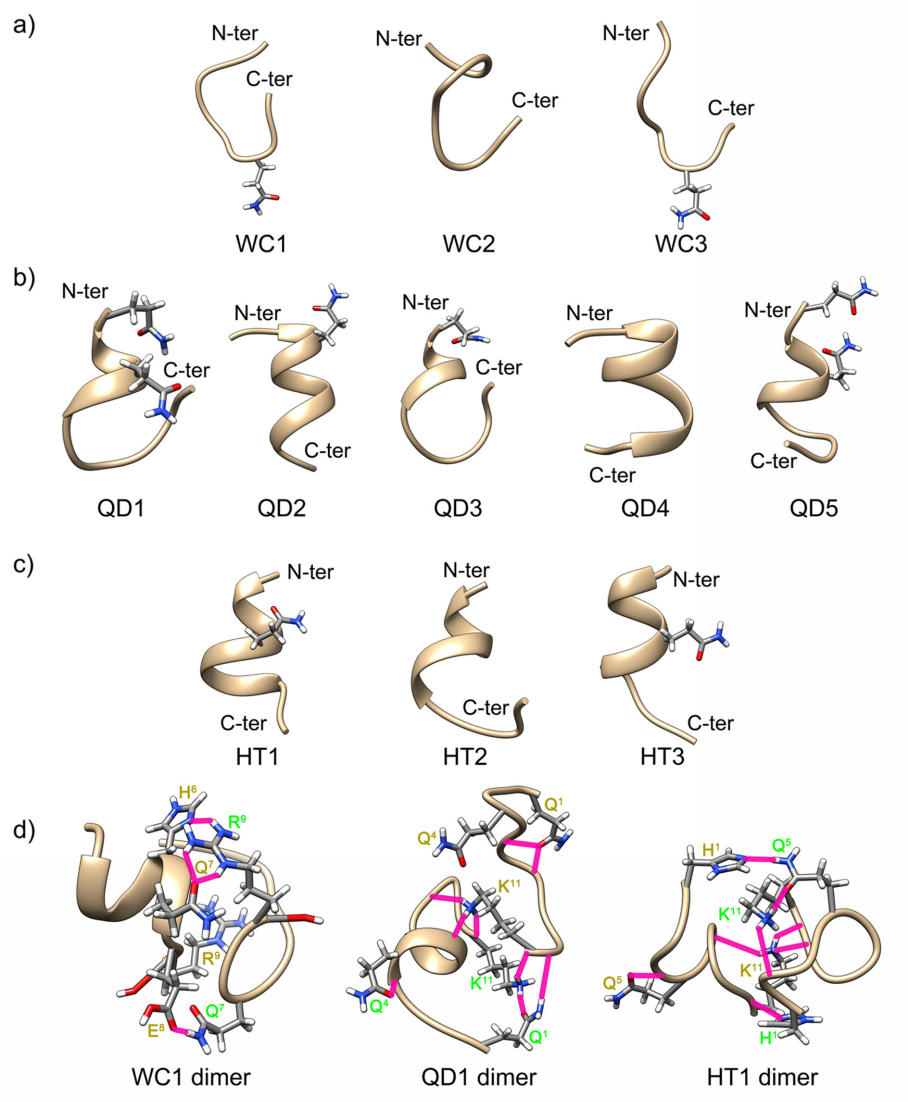

Figure 4. Structures of a) singly charged WC peptide ions, b) singly charged QD peptide ions, c) singly charged HT peptide ions, and dimers of the WC1/QD1/HT1 peptide ions. Side chains of glutamine and several amino acids are shown in this figure. The pink lines in Figure 4d show the hydrogen bonding of the side chains with other regions of the peptide.

additional evidence to support the above suggestion. Because the IM cell implemented in our IM-MS system (Waters Synapt G2-Si) is positioned after a trap collision cell, the peptide dimer ions generated by ESI are expected to be preserved in the trap. Thus, MS and MS/MS experiments were performed using the mixture of model peptide (WC1, QD1, and HT1) and its Ala→Val or Val→Ala mutant peptide (WC3, QD5, and HT3; Figure 3a) in order to prevent overlapping *m*/*z* values of the singly charged monomers and doubly charged dimers in the mass spectrum. Before performing the experiments, it was confirmed that WC3, QD5, and HT3 show singly charged monomeric ions in their mass spectra and high-mobility IM peaks in their IM distributions (Figure 3b and S7). The di-protonated dimeric ion formed between the model and mutant peptides was not observed in the mass spectrum (Figure 5a and S12). Nevertheless, isolation followed by collisional activation at target *m*/*z*, which corresponds to the di-protonated dimer of the model and mutant peptides, yielded singly protonated monomeric ions of the model and mutant peptides as CID products (Figure 5b and S12). This clearly supports that the model and mutant peptides form a di-protonated dimeric ion during the ESI process, which survived in the IM cell. Monomeric fragment ion peaks of the model and mutant peptides were observed even at a collision energy of 0 eV, indicating that the

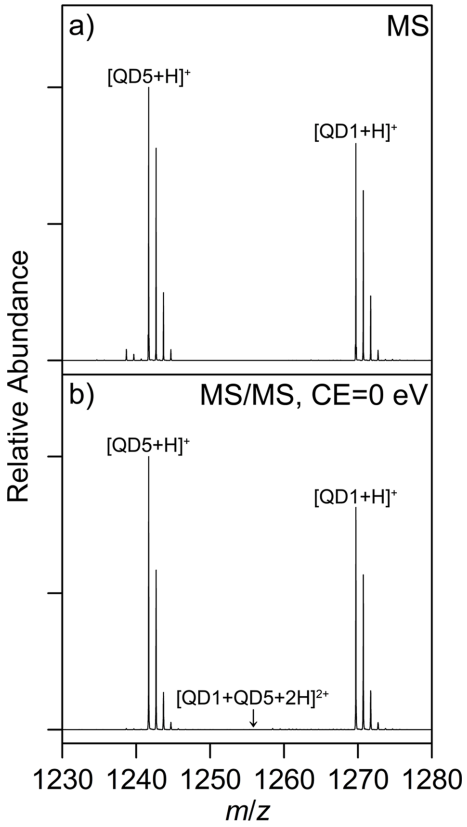

Figure 5. a) Mass and b) MS/MS spectrum of the QD1 and QD5 peptide mixture.

intermolecular interaction is very weak and transfer from the IM cell to the mass analyzer results in fragmentation of the complex ions into monomeric species. While we performed additional MS experiments which decrease the injection energies from IM cell to mass analyzer, the dimer peaks were not observed in mass spectra, estimating that is due to very weak intermolecular interactions. As a result, di-protonated dimeric ions were detected in the IM spectrum, but could not be detected in the MS spectrum. Systematic investigation revealed that the observed multiple IM peaks of the peptides containing Gln likely originate from multimeric complex ions, which is distinct from the formation of conformational isomers by Pro in the peptides.

Conclusions

The present study reveals that Gln is the second most abundant amino acid in the peptides with multiple IM peaks investigated herein, where 61.9% of the Gln-containing peptides give rise to multiple IM peaks. Mutant-based structural studies of Gln-containing peptides further suggest that the polar side chain of Gln promotes the formation of weakly bound peptide dimers during ESI, providing a unique mobility signature of the peptide ions. Overall, this study demonstrates that Gln in the peptide ion may be a key residue influencing the generation of multiple IM peaks for the peptide ion. We believe that our investigation of the distinct IM features of the peptides will greatly assist in the development of reliable ion mobility-based analytical techniques.

Supplementary Information

Supplementary information is available at https://docs.google.com/document/d/1nbFztZ9fOvYmaqgB80Ieyao3bT-gh_hW/edit?usp=sharing&ouid=111353140014732050956&rtpof=true&sd=true.

Acknowledgements

This research was supported by a National Research Council of Science & Technology (NST) grant from the Korean Government (MSIP) (No. CAP-15-10-KRICT) and a Korea University Future Research Grant.

Author Contributions

All authors contributed to the writing of the manuscript. All authors approved the final version of the manuscript.

Notes

The authors declare no competing financial interest.

References

1. Creaser, C. S.; Griffiths, J. R.; Bramwell, C. J.; Noreen, S.; Hill, C. A.; Thomas, C. L. P. *Analyst* **2004**, 129, 984, DOI: 10.1039/B404531A.
2. Kanu, A. B.; Dwivedi, P.; Tam, M.; Matz, L.; Hill Jr., H. H., *J. Mass Spectrom.* **2008**, 43, 1, DOI: 10.1002/jms.1383.
3. Lanucara, F.; Holman, S. W.; Gray, C. J.; Eyers, C. E. *Nat. Chem.* **2014**, 6, 281, DOI: 10.1038/nchem.1889.
4. May, J. C.; Goodwin, C. R.; Lareau, N. M.; Leaptrot, K. L.; Morris, C. B.; Kurulugama, R. T.; Mordehai, A.; Klein, C.; Barry, W.; Darland, E.; Overney, G.; Imatani, K.; Stafford, G. C.; Fjeldsted, J. C.; McLean, J. A. *Anal. Chem.* **2014**, 86, 2107, DOI: 10.1021/ac4038448.
5. Valentine, S.; Kulchania, M.; Barnes, C.; Clemmer, D. *Int. J. Mass Spectrom.* **2001**, 212, 97, DOI: 10.1016/S1387-3806(01)00511-5.
6. Campuzano, I.; Bush, M. F.; Robinson, C. V.; Beaumont, C.; Richardson, K.; Kim, H.; Kim, H. I. *Anal. Chem.* **2012**, 84, 1026, DOI: 10.1021/ac202625t.
7. McLean, J. A.; Ruotolo, B. T.; Gillig, K. J.; Russell, D. H. *Int. J. Mass Spectrom.* **2005**, 240, 301, DOI: 10.1016/j.ijms.2004.10.003.

8. Zhong, Y.; Hyung, S. J.; Ruotolo, B. T. *Expert Rev. Proteomics* **2012**, 9, 47, DOI: 10.1586/epr.11.75.
9. Creese, A. J.; Cooper, H. J. *Anal. Chem.* **2012**, 84, 2597, DOI: 10.1021/ac203321y.
10. Lietz, C. B.; Chen, Z.; Yun Son, C.; Pang, X.; Cui, Q.; Li, L. *Analyst* **2016**, 141, 4863, DOI: 10.1039/C5AN00835B.
11. Thalassinos, K.; Grabenauer, M.; Slade, S. E.; Hilton, G. R.; Bowers, M. T.; Scrivens, J. H. *Anal. Chem.* **2009**, 81, 248, DOI: 10.1021/ac801916h.
12. Counterman, A. E.; Clemmer, D. E. *Anal. Chem.* **2002**, 74, 1946, DOI: 10.1021/ac011083k.
13. Pierson, N. A.; Chen, L.; Russell, D. H.; Clemmer, D. E. *J. Am. Chem. Soc.* **2013**, 135, 3186, DOI: 10.1021/ja3114505.
14. Beckett, D.; El-Baba, T. J.; Clemmer, D. E.; Raghavachari, K. *J. Chem. Theory Comput.* **2018**, 14, 5406, DOI: 10.1021/acs.jctc.8b00648.
15. Masson, A.; Kamrath, M. Z.; Perez, M. A. S.; Glover, M. S.; Rothlisberger, U.; Clemmer, D. E.; Rizzo, T. R. *J. Am. Soc. Mass. Spectrom.* **2015**, 26, 1444, DOI: 10.1007/s13361-015-1172-4.
16. Warnke, S.; Baldauf, C.; Bowers, M. T.; Pagel, K.; von Helden, G. *J. Am. Chem. Soc.* **2014**, 136, 10308, DOI: 10.1021/ja502994b.
17. Bush, M. F.; Campuzano, I. D. G.; Robinson, C. V. *Anal. Chem.* **2012**, 84, 7124, DOI: 10.1021/ac3014498.
18. Hess, B.; Kutzner, C.; van der Spoel, D.; Lindahl, E. *J. Chem. Theory Comput.* **2008**, 4, 435, DOI: 10.1021/ct700301q.
19. Pronk, S.; Páll, S.; Schulz, R.; Larsson, P.; Bjelkmar, P.; Apostolov, R.; Shirts, M. R.; Smith, J. C.; Kasson, P. M.; van der Spoel, D.; Hess, B.; Lindahl, E. *Bioinformatics* **2013**, 29, 845, DOI: 10.1093/bioinformatics/btt055.
20. Vanommeslaeghe, K.; Hatcher, E.; Acharya, C.; Kundu, S.; Zhong, S.; Shim, J.; Darian, E.; Guvench, O.; Lopes, P.; Vorobyov, I.; Mackerell Jr., A. D. *J. Comput. Chem.* **2010**, 31, 671, DOI: 10.1002/jcc.21367.
21. Lee, H. H. L.; Heo, C. E.; Seo, N.; Yun, S. G.; An, H. J.; Kim, H. I. *J. Am. Chem. Soc.* **2018**, 140, 16528, DOI: 10.1021/jacs.8b07864.
22. Lee, H. H. L.; Kim, H. I. *Isr. J. Chem.* **2018**, 58, 472, DOI: 10.1002/ijch.201700073.
23. Mesleh, M. F.; Hunter, J. M.; Shvartsburg, A. A.; Schatz, G. C.; Jarrold, M. F. *J. Phys. Chem.* **1996**, 100, 16082, DOI: 10.1021/jp961623v.
24. Hall, Z.; Politis, A.; Bush, M. F.; Smith, L. J.; Robinson, C. V. *J. Am. Chem. Soc.* **2012**, 134, 3429, DOI: 10.1021/ja2096859.
25. Hudgins, R. R.; Jarrold, M. F. *J. Am. Chem. Soc.* **1999**, 121, 3494, DOI: 10.1021/ja983996a.
26. Shek, P. Y. I.; Zhao, J.; Ke, Y.; Siu, K. W. M.; Hopkinson, A. C. *J. Phys. Chem. A* **2006**, 110, 8282, DOI: 10.1021/jp055426k.
27. Tao, L.; McLean, J. R.; McLean, J. A.; Russell, D. H. *J. Am. Soc. Mass. Spectrom.* **2007**, 18, 1232, DOI: 10.1016/j.jasms.2007.04.003.
28. Hudgins, R. R.; Ratner, M. A.; Jarrold, M. F. *J. Am. Chem. Soc.* **1998**, 120, 12974, DOI: 10.1021/ja983021q.
29. Johnson, A. R.; Dilger, J. M.; Glover, M. S.; Clemmer, D. E.; Carlson, E. E. *Chem. Commun.* **2014**, 50, 8849, DOI: 10.1039/C4CC03257H.